2012

The metal ion-dependent adhesion site motif of the Enterococcus faecalis EbpA pilin mediates pilus function in catheter-associated urinary tract infection

Hailyn V. Nielsen
Washington University School of Medicine in St. Louis

Pascale S. Guiton
Washington University School of Medicine in St. Louis

Kimberly A. Kline
Washington University School of Medicine in St. Louis

Gary C. Port
Washington University School of Medicine in St. Louis

Jerome S. Pinkner
Washington University School of Medicine in St. Louis

See next page for additional authors

The Metal Ion-Dependent Adhesion Site Motif of the *Enterococcus faecalis* EbpA Pilin Mediates Pilus Function in Catheter-Associated Urinary Tract Infection

Hailyn V. Nielsen, Pascale S. Guiton, Kimberly A. Kline, et al.

2012. The Metal Ion-Dependent Adhesion Site Motif of the *Enterococcus faecalis* EbpA Pilin Mediates Pilus Function in Catheter-Associated Urinary Tract Infection . mBio 3(4): . doi:10.1128/mBio.00177-12.

The Metal Ion-Dependent Adhesion Site Motif of the *Enterococcus faecalis* EbpA Pilin Mediates Pilus Function in Catheter-Associated Urinary Tract Infection

Hailyn V. Nielsen,[a] Pascale S. Guiton,[a] Kimberly A. Kline,[a]* Gary C. Port,[a] Jerome S. Pinkner,[a] Fabrice Neiers,[b]* Staffan Normark,[b] Birgitta Henriques-Normark,[b] Michael G. Caparon,[a] and Scott J. Hultgren[a]

Department of Molecular Microbiology and Center for Women's Infectious Disease Research, Washington University School of Medicine, St. Louis, Missouri, USA,[a] and Department of Microbiology, Tumor Biology and Cell Biology, Karolinska Institute, Stockholm, Sweden[b]

* Present address: Kimberly A. Kline, Singapore Centre on Environmental Life Sciences Engineering, School of Biological Sciences, Nanyang Technological University, Singapore; Fabrice Neiers, Centre des Sciences du Goût et de l'Alimentation, UMR6265 CNRS, UMR1324 INRA, Université de Bourgogne, Dijon, France

ABSTRACT **Though the bacterial opportunist *Enterococcus faecalis* causes a myriad of hospital-acquired infections (HAIs), including catheter-associated urinary tract infections (CAUTIs), little is known about the virulence mechanisms that it employs. However, the endocarditis- and biofilm-associated pilus (Ebp), a member of the sortase-assembled pilus family, was shown to play a role in a mouse model of *E. faecalis* ascending UTI. The Ebp pilus comprises the major EbpC shaft subunit and the EbpA and EbpB minor subunits. We investigated the biogenesis and function of Ebp pili in an experimental model of CAUTI using a panel of chromosomal pilin deletion mutants. A nonpiliated pilus knockout mutant (EbpABC$^-$ strain) was severely attenuated compared to its isogenic parent OG1RF in experimental CAUTI. In contrast, a nonpiliated *ebpC* deletion mutant (EbpC$^-$ strain) behaved similarly to OG1RF *in vivo* because it expressed EbpA and EbpB. Deletion of the minor pilin gene *ebpA* or *ebpB* perturbed pilus biogenesis and led to defects in experimental CAUTI. We discovered that the function of Ebp pili *in vivo* depended on a predicted metal ion-dependent adhesion site (MIDAS) motif in EbpA's von Willebrand factor A domain, a common protein domain among the tip subunits of sortase-assembled pili. Thus, this study identified the Ebp pilus as a virulence factor in *E. faecalis* CAUTI and also defined the molecular basis of this function, critical knowledge for the rational development of targeted therapeutics.**

IMPORTANCE **Catheter-associated urinary tract infections (CAUTIs), one of the most common hospital-acquired infections (HAIs), present considerable treatment challenges for physicians. Inherently resistant to several classes of antibiotics and with a propensity to acquire vancomycin resistance, enterococci are particularly worrisome etiologic agents of CAUTI. A detailed understanding of the molecular basis of *Enterococcus faecalis* pathogenesis in CAUTI is necessary for the development of preventative and therapeutic strategies. Our results elucidated the importance of the *E. faecalis* Ebp pilus and its subunits for enterococcal virulence in a mouse model of CAUTI. We further showed that the metal ion-dependent adhesion site (MIDAS) motif in EbpA is necessary for Ebp function *in vivo*. As this motif occurs in other sortase-assembled pili, our results have implications for the molecular basis of virulence not only in *E. faecalis* CAUTI but also in additional infections caused by enterococci and other Gram-positive pathogens.**

Received 7 June 2012 **Accepted** 11 June 2012 **Published** 24 July 2012

Citation Nielsen HV, et al. 2012. The metal ion-dependent adhesion site motif of the *Enterococcus faecalis* EbpA pilin mediates pilus function in catheter-associated urinary tract infection. mBio 3(4):e00177-12. doi:10.1128/mBio.00177-12.

Editor R. John Collier, Harvard Medical School

Address correspondence to Scott J. Hultgren, hultgren@borcim.wustl.edu, or Michael G. Caparon, caparon@borcim.wustl.edu.

In recent decades, *Enterococcus faecalis* and *Enterococcus faecium*, commensal gut bacteria, have emerged as human pathogens (1). Enterococci frequently cause hospital-acquired and device-associated infections, including bloodstream infections, infective endocarditis, and catheter-associated urinary tract infections (CAUTIs) (2). As the most common hospital-acquired infection (HAI) (3) and because they are frequently and often unnecessarily treated with antibiotics (4), CAUTIs are a reservoir of nosocomial and antimicrobial-resistant pathogens (5). Due to the tremendous incidence of CAUTI, infrequent but life-threatening sequelae such as bacteremia and urosepsis are significant complications (6). Enterococci are responsible for roughly 15% of CAUTIs (7). The recent surge of enterococcal infections correlates with both their inherent and acquired antimicrobial resistances, including vancomycin resistance (2). Both rising antimicrobial resistance and bacterial biofilm formation on indwelling catheters, abiotic surfaces protected from host immune responses and antibiotics, contribute to the difficulty associated with successful CAUTI treatment. Thus, a better understanding of bacterial pathogenesis in CAUTI is critical for the development of preventative and therapeutic antimicrobial agents.

Among the few described enterococcal virulence factors is the

endocarditis- and biofilm-associated pilus (Ebp) (8). The Ebp pilus is an example of the sortase-assembled pilus family, whose members are now described among diverse Gram-positive genera, including *Corynebacterium* (9), *Actinomyces* (10), *Streptococcus* (11–13), *Bacillus* (14), *Enterococcus* (8, 15, 16), *Lactobacillus* (17), and *Bifidobacterium* (18). Sortase-assembled pili consist of a major pilin subunit and up to two minor subunits, each with a C-terminal cell wall sorting signal (CWSS) that includes an LPXTG-like sortase recognition motif (19). One or more genetically linked membrane-associated transpeptidase enzymes, pilus-associated sortases, catalyze the formation of interpilin isopeptide bonds found in mature pili (20). Repeating, covalently linked major pilin subunits comprise the bulk of the pilus fiber. When present, a second minor subunit is proposed to localize to the fiber tip and a third subunit is proposed to localize to the base (19). Respectively, these ancillary pilins may facilitate interaction with host proteins and the anchoring of pilus fibers to the cell wall via processing by the housekeeping sortase. Though dispensable for major pilin polymerization, minor subunits have been shown to affect aspects of pilus biogenesis, including pilus length, thickness, and subcellular compartmentalization in several sortase-assembled pilus systems (21, 22). Characteristically, the *E. faecalis ebp* operon encodes three structural proteins, EbpA, EbpB, and EbpC, and the pilus-associated sortase SrtC (or Bps) (8). A housekeeping sortase, SrtA, is encoded elsewhere in the genome (23). Ebp pilus fibers consist largely of the major pilin EbpC, whose polymerization is mediated by SrtC. EbpA and EbpB are covalently incorporated into the cell wall-anchored Ebp pilus fibers as minor components (8), but their roles in pilus biogenesis and pilus function have not been directly investigated previously.

Sortase-assembled pili or their subunits have been reported as virulence factors *in vivo* in infection models of group B streptococci (GBS; *Streptococcus agalactiae*) (24–26), group A streptococci (GAS; *Streptococcus pyogenes*) (27, 28), and the pneumococcus (*Streptococcus pneumoniae*) (13). A polar, nonpiliated *E. faecalis ebp* mutant was attenuated in animal models of infective endocarditis (8) and ascending UTI (29), as were *E. faecalis* mutants lacking SrtC or SrtA (30) and a nonpiliated *E. faecium ebp* mutant (31). A mutant lacking SrtA was also attenuated in the model of CAUTI used in this study (32), but the role of Ebp pili in CAUTI has not been directly investigated. Though the function of Ebp pili in pathogenesis is unclear, *in vitro* studies suggested that Ebp pili were important for static biofilm formation (8) and adherence to extracellular matrix (ECM) proteins (33) and human platelets (34). However, the unique contributions of EbpA, EbpB, or EbpC to any described Ebp pilus function have not been explored.

In this report, we hypothesized that the Ebp pilus is a virulence factor in CAUTI. To test this hypothesis, we investigated its importance for *E. faecalis* pathogenesis in a mouse model that mimics many aspects of human CAUTI (32). We evaluated the role of each Ebp structural subunit in pilus biogenesis and in virulence in CAUTI, revealing that the minor pilins mediated pilus function *in vivo*. Specifically, the metal ion-dependent adhesion site (MIDAS) motif in EbpA's predicted von Willebrand factor A (VWA) domain, a common domain among sortase-assembled pili (22), was critical for *E. faecalis* virulence in CAUTI. Thus, this study elucidated the molecular basis of Ebp pilus function in experimental *E. faecalis* CAUTI.

RESULTS

Ebp pili are important in a mouse model of CAUTI. We used a previously described mouse model of *E. faecalis* CAUTI (32) and a chromosomal deletion mutant lacking all three Ebp structural pilins (EbpABC$^-$ strain) to investigate the importance of Ebp pili in pathogenesis. Bladders of female mice were implanted with a short segment of silicone tubing (implant) to mimic urinary catheterization and subsequently infected with the *E. faecalis* OG1RF or EbpABC$^-$ strain. Twenty-four hours postinfection (p.i.), the bacterial burdens in the bladders and those associated with the implants were determined as a measure of virulence. Median CFU recovered from the bladders (Fig. 1A) and implants (Fig. 1B) of mice infected with the EbpABC$^-$ strain were significantly lower than those recovered from the bladders and implants of mice infected with OG1RF. These results demonstrated that Ebp pili were important for *E. faecalis* pathogenesis in experimental CAUTI.

To identify the functional subunit critical for pilus-mediated virulence in CAUTI, we created a panel of unmarked, in-frame single and double pilin deletion mutants. In the initial steps of this analysis, we evaluated (i) EbpC assembly and expression in minor pilin deletion mutants (EbpA$^-$, EbpB$^-$, and EbpAB$^-$ strains) and (ii) expression of minor pilin(s) in nonpiliated *ebpC* deletion mutants (EbpC$^-$, EbpBC$^-$, and EbpAC$^-$ strains).

Expression of EbpA and EbpB in the absence of pilus fibers. EbpC is the major pilus subunit necessary for fiber polymerization (8). Thus, we evaluated minor pilin expression in the absence of EbpC in Western blot analyses using anti-EbpA and anti-EbpB sera after reducing SDS-PAGE. In EbpC$^-$ cell lysates, we observed two EbpA doublets migrating at approximately 140 kDa and 100 kDa (Fig. 2A, open arrowhead and asterisk, respectively). We observed only one EbpB species migrating at a size similar to the larger ~140-kDa EbpA species (Fig. 2B, open arrowhead). Because the ~140-kDa species recognized by both anti-EbpA and anti-EbpB sera was larger than the predicted molecular masses for either EbpA or EbpB monomer after cleavage of its signal sequence and CWSS (~120 and ~46 kDa, respectively), we hypothesized that this species likely represents an EbpA-EbpB heterodimer. As formation of autocatalytic intramolecular isopeptide bonds has been shown to change the mobility of other sortase-assembled pilus subunits on SDS-PAGE (35), we predict that the ~100-kDa EbpA species is the fully processed EbpA monomer.

To test this hypothesis, we analyzed EbpA and EbpB expression in a mutant lacking all sortase genes (SrtC$^-$ SrtA$^-$ strain) to prevent formation of interpilin isopeptide bonds. In Western blots of SrtC$^-$ SrtA$^-$ cell lysates, the ~100-kDa EbpA species predominated (Fig. 2A, asterisk). The same result was obtained with our SrtC$^-$ mutant (data not shown), consistent with prior reports for OG1RF (8) and *E. faecalis* OG1X (36). Furthermore, we observed the ~100-kDa EbpA species in cell lysates of the EbpBC$^-$ strain (Fig. 2A, asterisk).

The ~140-kDa species was also absent when anti-EbpB sera were used to probe Western blots of SrtC$^-$ SrtA$^-$ (Fig. 2B and 2C), SrtC$^-$ (data not shown), and EbpAC$^-$ (Fig. 2B and 2C) strains. In these strains, EbpB migrated just below the 50-kDa protein marker, consistent with its predicted monomer size (Fig. 2B and 2C, hash marks). Thus, formation of the ~140-kDa EbpA and EbpB species observed in the EbpC$^-$ strain depended on EbpB and EbpA, respectively, and SrtC, consistent with the formation of an EbpA-EbpB heterodimer. Interestingly, we found EbpB mono-

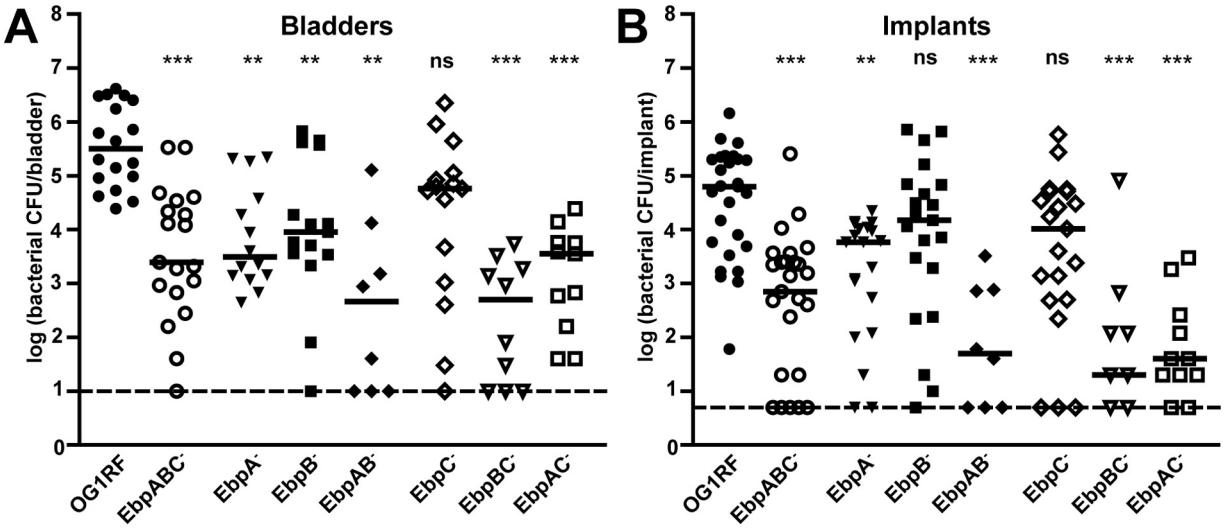

FIG 1 Virulence of *E. faecalis* OG1RF and its isogenic pilin deletion mutants in experimental CAUTI. Twenty-four-hour viable bacterial titers in the bladders (A) and those associated with implants (B) from 2 to 4 independent experiments/strain are shown. Each shape corresponds to one mouse; open shapes represent nonpiliated bacterial strains. Median titers (CFU/bladder, CFU/implant) are shown with a bar: OG1RF (3.20×10^5, 6.25×10^4), EbpABC$^-$ strain (2.48×10^3, 7.00×10^2), EbpA$^-$ strain (3.10×10^3, 5.82×10^3), EbpB$^-$ strain (9.08×10^3, 1.50×10^4), EbpAB$^-$ strain (4.60×10^2, 50), EbpC$^-$ strain (5.80×10^4, 1.04×10^4), EbpBC$^-$ strain (5.00×10^2, 20), and EbpAC$^-$ strain (3.56×10^3, 40). Dashed lines are the limits of detection (10 CFU/bladder, 5 CFU/implant). Results of statistical comparisons of each mutant to OG1RF for bladders and implants are shown. There were no significant differences in bladder or implant colonization between any double pilin deletion mutant and the EbpABC$^-$ strain (data not shown). *P* values were adjusted for 10 comparisons (**, $P < 0.01$; ***, $P < 0.001$; ns, not significant).

mers in the culture supernatants of OG1RF (Fig. 3B) and pilin deletion mutants: EbpA$^-$ (Fig. 3B) and EbpC$^-$ and EbpAC$^-$ (Fig. 2C) strains. However, in the SrtC$^-$ SrtA$^-$ mutant, EbpB monomers were observed only in cell lysates (Fig. 2B), suggesting sortase-dependent dissociation of EbpB monomers from bacterial cells.

Finally, complementation of the EbpABC$^-$ strain with *ebpA*, *ebpB*, and *ebpC* provided in *trans* resulted in incorporation of EbpA and EbpB into high-molecular-weight pilus ladders (HMWLs) in cell wall fractions, similar to those seen in OG1RF (Fig. 2D and 2E, respectively). However, when the EbpABC$^-$ strain was provided with only *ebpA* and *ebpB* in *trans*, EbpA and EbpB expression mirrored that seen in the EbpC$^-$ strain: ~140-kDa and ~100-kDa EbpA species (Fig. 2D, open arrowhead and asterisk) and ~140-kDa EbpB species (Fig. 2E, open arrowhead). Taken together, these data suggest that an EbpA-EbpB heterodimer is formed by SrtC and anchored to the cell wall in the absence of EbpC.

Chromosomal deletion of minor pilins perturbs Ebp biogenesis. Others have observed that deletion of minor subunits from other sortase-assembled pilus islands can affect aspects of pilus biogenesis, including morphology and population piliation dynamics. Thus, we analyzed pilus biogenesis in the EbpA$^-$, EbpB$^-$, and EbpAB$^-$ minor pilin deletion mutants using anti-EbpC sera. Western blots showed that deletion of either *ebpA* or *ebpB* did not prevent expression of EbpC (Fig. 3A and 3C, respectively) or expression of the remaining minor subunit (Fig. 3B and 3D, respectively). However, the EbpC species detected in EbpA$^-$ and EbpAB$^-$ cell lysates was a compressed band that barely migrated into gels (Fig. 3A). This differed from the EbpC pilus HMWL observed in OG1RF. In contrast, EbpC HMWLs from the EbpB$^-$ and OG1RF strains were indistinguishable (Fig. 3C). To test whether *ebpA* provided in *trans* could restore OG1RF-like EbpC HMWLs in EbpA$^-$ and EbpAB$^-$ strains, *ebpA* was placed under the control of a tetracycline-inducible promoter on a plasmid. High- and low-level EbpA expression was observed from this plasmid with induction (100 μg ml^{-1} anhydrotetracycline) and no induction, respectively, in the EbpABC$^-$ strain. However, EbpA expressed from this plasmid with or without induction was not incorporated into and did not affect compressed EbpC bands in the EbpA$^-$ and EbpAB$^-$ strains (data not shown). Thus, compressed EbpC bands caused by deletion of *ebpA* indicated altered pilus morphology that could not be complemented in *trans*.

We next investigated pilus morphology in minor pilin deletion mutants using deep-etch immunogold electron microscopy (EM). In the OG1RF and EbpB$^-$ strains, multiple pilus fibers several hundred nanometers long were observed associated with bacterial cells (Fig. 3E, arrowheads). In contrast, in cultures of the EbpA$^-$ and EbpAB$^-$ strains, we observed fewer but much longer EbpC fibers (greater than 1 μm) associated with some cells (Fig. 3E, large arrows). An analysis of population piliation dynamics using immunofluorescence microscopy (IFM) also revealed defects of the minor pilin deletion strains in pilus biogenesis. A significantly smaller median proportion of EbpA$^-$, EbpB$^-$, and EbpAB$^-$ bacterial cells (1.1%, 33.9%, and 2.8%, respectively) expressed EbpC at their surface than did OG1RF (65.8%) (Fig. 3F). Thus, deletion of minor pilin coding sequences in OG1RF affected Ebp pilus biogenesis.

Minor pilin deletion mutants are attenuated in experimental *E. faecalis* CAUTI. We then investigated the minor pilin deletion mutants in experimental CAUTI. EbpA$^-$, EbpB$^-$, and EbpAB$^-$ strains were all significantly attenuated in bladder colonization compared to OG1RF (Fig. 1A). EbpA$^-$ and EbpAB$^-$ strains were also attenuated in implant colonization (Fig. 1B). The defect of

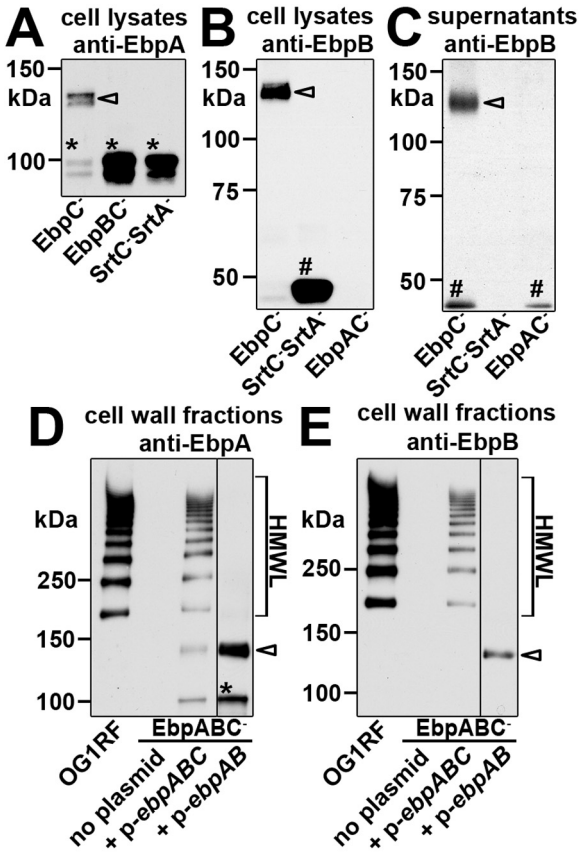

FIG 2 EbpA and EbpB expression in nonpiliated strains. Western blot analyses were performed after SDS-PAGE of the indicated bacterial strains and fractions using anti-EbpA (A and D) or anti-EbpB (B, C, and E) sera. Open arrowheads indicate the ~140-kDa EbpA and EbpB species observed in the EbpC$^-$ strain (A to C) and the EbpABC$^-$/p-*ebpAB* strain (D and E). Asterisks show the ~100-kDa EbpA monomer in EbpC$^-$, EbpBC$^-$, and SrtC$^-$ SrtA$^-$ strains (A) and in the EbpABC$^-$/p-*ebpAB* strain (D). Hash marks show the EbpB monomer in EbpC$^-$, EbpAC$^-$, and SrtC$^-$ SrtA$^-$ strains (B and C) and in the EbpABC$^-$/p-*ebpAB* strain (E). Brackets indicate pilus HMWLs observed in OG1RF and the EbpABC$^-$/p-*ebpABC* strain.

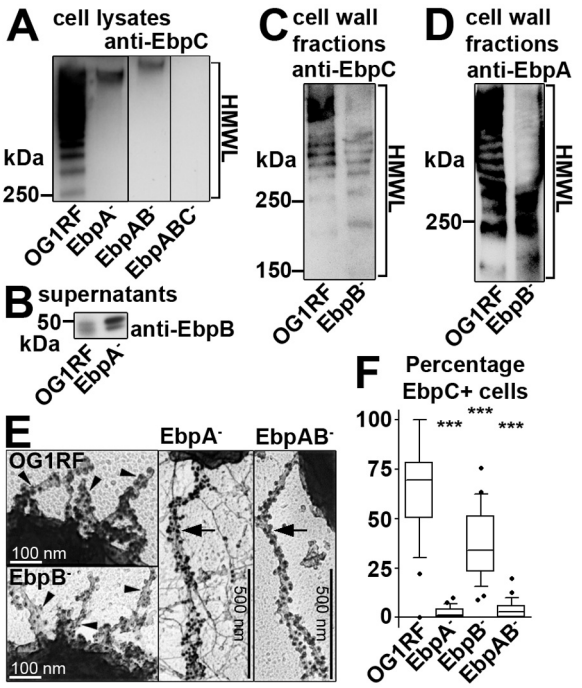

FIG 3 Minor pilin deletions affect pilus biogenesis. Anti-EbpC sera were used to assess pilus assembly by Western blot analysis (A to D), to visualize pilus morphology with deep-etch EM (E), and to evaluate population piliation dynamics by IFM (F). (A) Western blot analysis of EbpA$^-$ and EbpAB$^-$ cell lysates showed condensed EbpC bands with reduced mobility on SDS-PAGE compared to OG1RF EbpC HMWL. (B) EbpB is expressed in OG1RF and EbpA$^-$ culture supernatants. (C and D) EbpC HMWL (C) and EbpA HMWL (D) in EbpB$^-$ and OG1RF strains were similar. HMWLs (brackets) indicate pilus polymerization (anti-EbpC) or minor pilin incorporation (anti-EbpA). (E) Pilus morphology was altered in EbpA$^-$ and EbpAB$^-$ strains. Arrowheads point to gold bead-labeled pilus fibers in OG1RF and EbpB$^-$ strains. Large arrows indicate gold bead-labeled long EbpC fibers in EbpA$^-$ and EbpAB$^-$ strains. (F) The percentage of bacterial cells expressing EbpC (EbpC$^+$ cells) was quantified in 3 independent experiments. The median percentages of EbpC$^+$ cells for each strain were determined: OG1RF (69.6), EbpA$^-$ strain (1.1), EbpB$^-$ strain (33.9), and EbpAB$^-$ strain (2.8). Whiskers show the 10th and 90th percentiles; dots show outliers. Statistically significant differences between OG1RF and each mutant strain are shown; *P* values were adjusted for 3 comparisons (***, $P < 0.001$).

these strains *in vivo* may have been due to the lack of EbpA and/or EbpB or to the effects of the minor pilin deletions on pilus biogenesis described in the studies above.

Expression of EbpA and EbpB in the EbpC$^-$ strain is sufficient for pilus-mediated virulence in CAUTI. Interestingly, the nonpiliated EbpC$^-$ mutant and OG1RF colonized the bladders and implants of infected mice to similar levels (Fig. 1A and 1B), demonstrating that EbpC and pilus fibers were dispensable for virulence in experimental *E. faecalis* CAUTI. This result suggested that the EbpA-EbpB ~140-kDa species, the ~100-kDa EbpA monomer, or the ~50-kDa EbpB monomer expressed in the EbpC$^-$ strain (Fig. 2A to 2C) was sufficient to mediate *E. faecalis* bladder and implant colonization. To investigate this further, we tested our nonpiliated mutants that expressed pilin monomer(s) but not the EbpA-EbpB heterodimer. In contrast to the EbpC$^-$ strain, median bladder and implant titers from mice infected with EbpBC$^-$ and EbpAC$^-$ strains were significantly lower than those from mice infected with OG1RF (Fig. 1A and 1B), showing that neither the EbpA nor the EbpB monomer alone was sufficient for pilus-mediated virulence in experimental CAUTI. Furthermore, we observed a similar defect in bladder and implant colonization by the SrtC$^-$ strain (Fig. 4A and 4B), which expresses both EbpA and EbpB monomers but lacks the EbpA-EbpB ~140-kDa species, further supporting a role for the EbpA-EbpB complex in pilus function in CAUTI.

Mutation of EbpA's MIDAS motif does not affect pilus biogenesis. Protein domain prediction revealed Cna B domains in the minor pilins and a von Willebrand factor A (VWA) domain with a metal ion-dependent adhesion site (MIDAS) motif (Asp-Xaa-Ser-Xaa-Ser. . . Thr. . . Asp) (37) in EbpA. To explore the importance of this motif in Ebp pilus function, we mutated predicted metal ion-coordinating residues of EbpA's MIDAS motif (Asp^{315}-Trp-Ser^{317}-Gly-Ser^{319}) to Ala (Ala^{315}-Trp-Ala^{317}-Gly-Ala^{319}) and assessed the effect of the mutations on pilus biogenesis and virulence in experimental CAUTI. When a mutant lacking all pilus subunits and *srtC* (EbpABC$^-$ SrtC$^-$ strain) was transformed with a plasmid carrying the *ebpABCsrtC* locus with a mutated MIDAS motif (p-*ebpA*^{AWAGA}*BCsrtC*), EbpC pilus fibers expressed

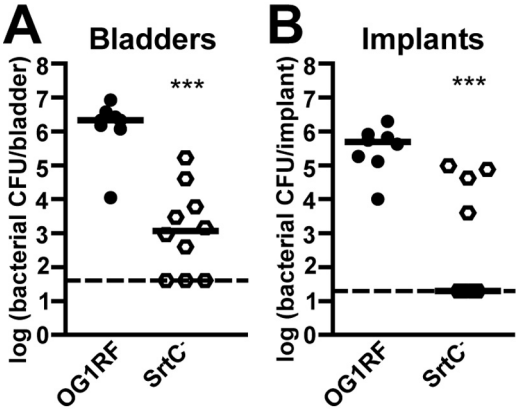

FIG 4 The SrtC$^-$ mutant is attenuated in experimental CAUTI. Mice were infected with ~2 × 10^7 CFU of OG1RF (closed circles) or the nonpiliated SrtC$^-$ mutant (open hexagons). Bacterial titers 24 h p.i. in the bladders (A) and implants (B) from 2 independent experiments are shown. Each shape corresponds to one mouse. Median titers (CFU/bladder, CFU/implant) are shown with a bar: OG1RF (2.16 × 10^6, 4.90 × 10^5) and SrtC$^-$ strain (1.18 × 10^3, 20). Dashed lines are limits of detection (40 CFU/bladder; 20 CFU/implant). Statistically significant differences between OG1RF and SrtC$^-$ titers are shown (***, $P < 0.001$).

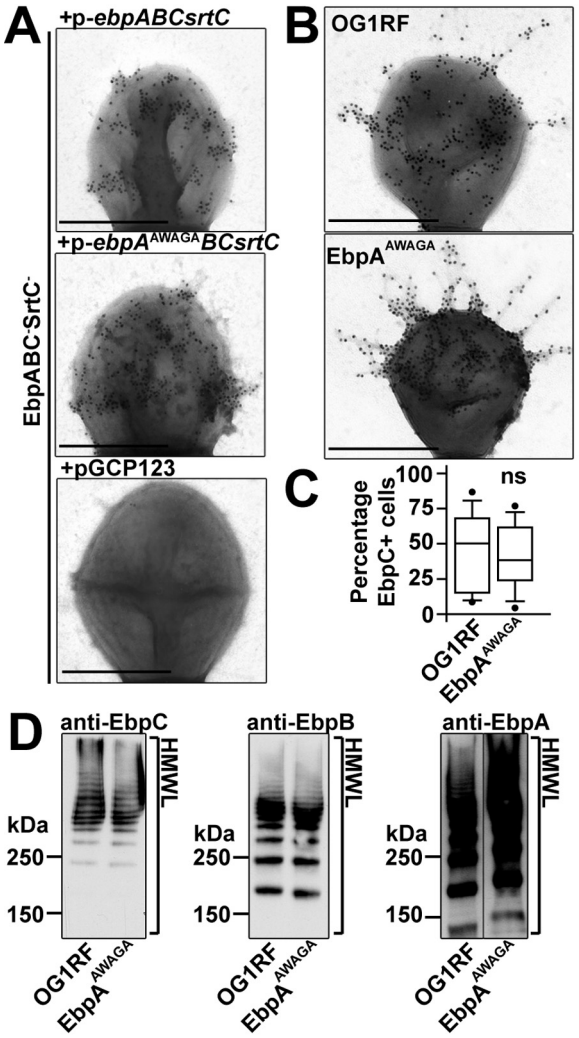

FIG 5 Mutation of EbpA's MIDAS motif does not affect pilus biogenesis. Mouse anti-EbpC polyclonal sera were used to assess pilus biogenesis by negative-stain immunogold EM (A and B), IFM (C), and Western blot analysis (D) after SDS-PAGE of the indicated cell fractions. (A and B) Piliation of the MIDAS motif mutant strains (EbpABC$^-$ SrtC$^-$/p-*ebpA*^{AWAGA}*BCsrtC* strain and EbpA^{AWAGA}) was similar to that of control strains (EbpABC$^-$ SrtC$^-$/p-*ebpABCsrtC* strain and OG1RF, respectively). Bars, 500 nm. (C) Comparison of the median percentages of EbpC$^+$ bacterial cells in OG1RF (50%) and EbpA^{AWAGA} (38%) from 2 independent experiments revealed no significant differences in population piliation dynamics. Whiskers show the 10th and 90th percentiles; dots show outliers (ns, not significant). (D) Pilus HMWLs on Western blots of OG1RF and EbpA^{AWAGA} probed with anti-EbpC (left), anti-EbpB (middle), and anti-EbpA (right) sera were indistinguishable.

by the resultant strain were similar to those observed from the EbpABC$^-$ SrtC$^-$ strain complemented with the unmutated OG1RF locus (p-*ebpABCsrtC*) as determined by negative-stain immunogold EM (Fig. 5A). We next introduced the mutant MIDAS motif into the chromosomal *ebpA* locus in OG1RF. Pili produced by this MIDAS mutant (EbpA^{AWAGA}) and by OG1RF were also similar when examined with negative-stain immunogold EM (Fig. 5B). Similarly, no difference between EbpA^{AWAGA} and OG1RF was observed in an IFM analysis of population piliation dynamics (Fig. 5C). Furthermore, HMWLs of EbpA^{AWAGA} and OG1RF were indistinguishable on Western blots probed with any antipilin immune serum (Fig. 5D). Thus, mutating EbpA's MIDAS motif did not affect pilus biogenesis.

EbpA MIDAS motif mutants are attenuated in experimental CAUTI. We next examined MIDAS motif mutants in experimental *E. faecalis* CAUTI. There were no significant differences between the median 24-h bladder or implant bacterial titers of mice infected with strains expressing pili with unmodified MIDAS motifs: OG1RF/pGCP123 (empty vector) and EbpABC$^-$ SrtC$^-$/p-*ebpABCsrtC* strain. Twenty-four-hour bacterial titers from mice infected with the nonpiliated EbpABC$^-$ SrtC$^-$/pGCP123 strain and with the EbpABC$^-$ SrtC$^-$/p-*ebpA*^{AWAGA}*BCsrtC* MIDAS motif mutant also did not differ significantly from each other. However, infections with either of these strains resulted in significantly lower bladder and implant bacterial burdens 24 h p.i. than those of OG1RF/pGCP123 or the EbpABC$^-$ SrtC$^-$/p-*ebpABCsrtC* strain (Fig. 6A and 6B). Thus, supplying the OG1RF *ebpABCsrtC* locus to the EbpABC$^-$ SrtC$^-$ strain in *trans* fully complemented its virulence defect in CAUTI, while provision of an *ebpA*^{AWAGA}*BCsrtC* mutant MIDAS motif locus in *trans* resulted in attenuation in CAUTI similar to that seen with provision of the empty vector alone.

Similarly, when we implanted and infected mice with the chromosomal MIDAS motif mutant (EbpA^{AWAGA}) and monitored the bacterial burdens both 24 h (Fig. 7A and 7B) and 7 days (Fig. 7C and 7D) p.i., the EbpA^{AWAGA} and EbpABC$^-$ strains were similarly attenuated in both bladder (Fig. 7A and 7C) and implant (Fig. 7B and 7D) colonization at each time point tested compared to OG1RF, revealing that EbpA's MIDAS motif is necessary for Ebp pilus function in experimental *E. faecalis* CAUTI.

Ebp pilus importance in UTI is tissue and model specific. There were no significant differences between the median bacterial kidney titer of mice infected with any pilin mutant and that of mice infected with OG1RF at any time point in experimental CAUTI (see Fig. S1 in the supplemental material). Thus, the importance of Ebp pili in this model was specific to implants and

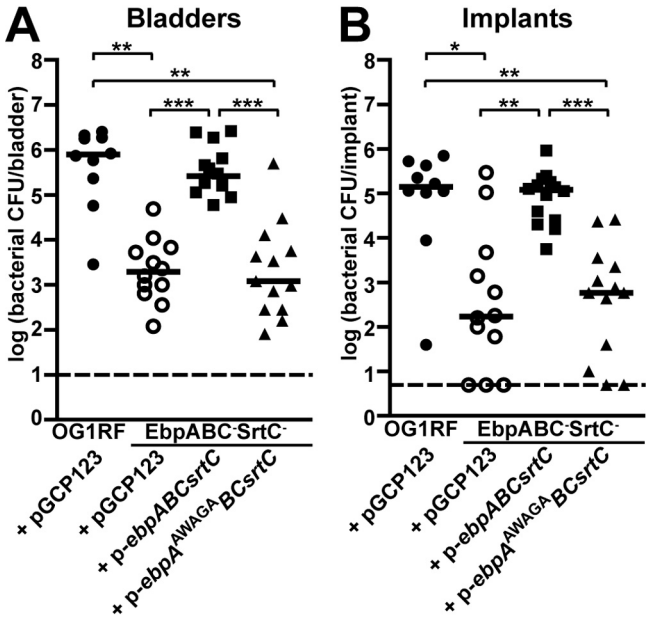

FIG 6 Transformation of EbpABC$^-$ SrtC$^-$ strain with p-*ebpABCsrtC* but not p-*ebpA*^{AWAGA}*BCsrtC* or pGCP123 complemented its virulence defect in experimental CAUTI. Bacterial titers 24 h p.i. of the bladders (A) and implants (B) from 2 independent experiments are shown. Each shape corresponds to one mouse; open shapes represent a nonpiliated bacterial strain. Median titers (CFU/bladder, CFU/implant) are shown with a bar: OG1RF/pGCP123 (5.92×10^5, 1.96×10^5), EbpABC$^-$ SrtC$^-$/pGCP123 strain (1.94×10^3, 1.72×10^2), EbpABC$^-$ SrtC$^-$/p-*ebpABCsrtC* strain (2.60×10^5, 1.20×10^5), and EbpABC$^-$ SrtC$^-$/p-*ebpA*^{AWAGA}*BC* strain (1.20×10^3, 5.80×10^2). Dashed lines are the limits of detection (10 CFU/bladder, 5 CFU/implant). All possible strain pairs were compared statistically. *P* values were adjusted for 6 comparisons. Significant differences are shown (*, $P < 0.05$; **, $P < 0.01$; ***, $P < 0.001$).

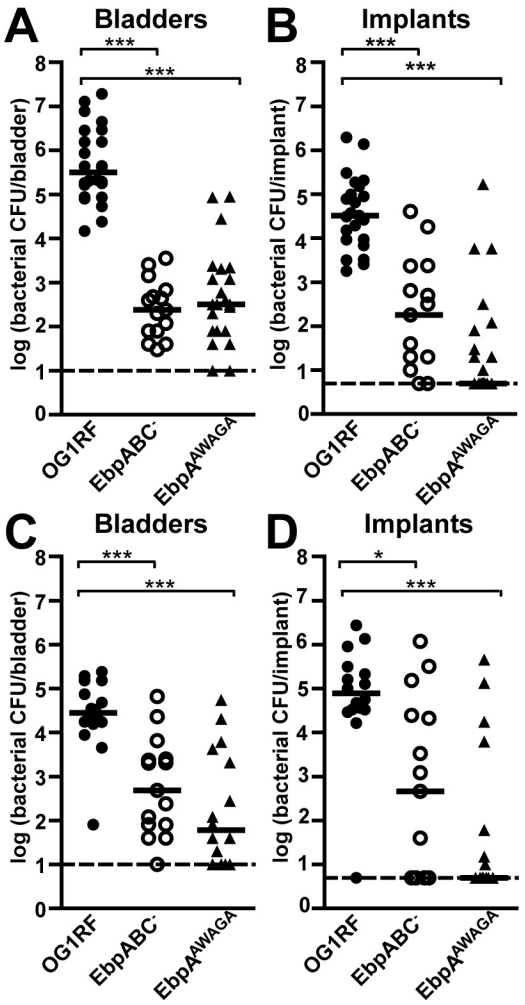

FIG 7 The chromosomal MIDAS mutant (EbpA^{AWAGA}) was as attenuated as the EbpABC$^-$ strain in experimental CAUTI. Twenty-four-hour (A and B) or 7-day (C and D) viable bacterial counts from the bladders (A and C) and implants (B and D) of mice infected with *E. faecalis* were pooled from 2 to 3 independent experiments for each strain. Each shape corresponds to one mouse; open shapes represent a nonpiliated bacterial strain. Median bacterial titers (CFU/bladder, CFU/implant) were determined at 24 h p.i. for OG1RF (3.16×10^5, 3.24×10^4), EbpA^{AWAGA} (2.40×10^2, 1.80×10^2), and EbpABC$^-$ (3.20×10^2, 5) strains and at 7 days for OG1RF (2.82×10^4, 7.86×10^4), EbpA^{AWAGA} (4.80×10^2, 4.60×10^2), and EbpABC$^-$ (60, 5) strains. Bars are medians; dashed lines are the limits of detection (10 CFU/bladder, 5 CFU/implant). All possible strain combinations were compared statistically; *P* values were adjusted for 3 comparisons. Significant differences are shown (*, $P < 0.05$; ***, $P < 0.001$).

implanted bladders. To further investigate the tissue specificity of Ebp pili, we compared the EbpABC$^-$ and EbpC$^-$ strains to OG1RF in a previously described mouse model of ascending UTI (38) in which *E. faecalis* displays kidney tropism (see Text S1 for methods). Since growth in serum was reported to increase expression of Ebp pili (8), we tested two inoculum preparation methods: bacterial subculture in brain heart infusion (BHI) broth alone or that in BHI broth with 40% horse serum. Each mutant fared as well as or better than OG1RF in bladders and kidneys at both 6 h and 48 h p.i. using either inoculum preparation method (see Fig. S2 in the supplemental material). Thus, Ebp pili were dispensable for *E. faecalis* virulence in our model of ascending UTI using mice of the same age and genetic background as those used in our model of CAUTI (7- to 8-week-old C57BL/6 mice). Consistent with the model specificity of Ebp pili in UTI pathogenesis observed here, Singh et al. previously showed a defect for a polar, nonpiliated *ebp* mutant in a different model of ascending UTI using younger, outbred mice, different bacterial inoculum preparation methods, and distinct virulence metrics (29).

DISCUSSION

In this study, we demonstrated a specific role for Ebp pili in a newly characterized mouse model of *E. faecalis* CAUTI. To investigate the molecular basis of pilus function *in vivo*, we described the effects of an extensive panel of pilus structural subunit deletions on both pilus biogenesis and pilus function in experimental CAUTI. Finally, we showed that EbpA and the MIDAS motif encoded by its predicted VWA domain were critical for pilus-mediated virulence *in vivo*, thus defining the molecular basis of pilus function in experimental *E. faecalis* CAUTI.

The EbpABC$^-$ mutant lacking all structural subunits was severely attenuated in bladder and implant colonization in experimental CAUTI, showing that the Ebp pilus was an important virulence factor in this model. The residual bladder and implant colonization by the EbpABC$^-$ strain suggests that additional bacterial factors may play a role in *E. faecalis* CAUTI. To investigate

the molecular basis of pilus function *in vivo*, we characterized a panel of pilin deletion mutants. We found that deletion of *ebpA* altered pilus morphology, leading to extended EbpC fibers. Similarly, deletion of either the *pilA* or *pilC* minor pilin gene from the GBS NEM316 pilus island 2A (PI-2A) led to longer pilus fibers (22). In *Corynebacterium diphtheriae*, mutants lacking the minor anchor pilin (SpaB) produced longer pilus fibers, presumably because cell wall anchoring achieved via SpaB processing by the housekeeping sortase prevents further polymerization by the pilus-associated sortase (21, 39). However, pili of our mutant lacking EbpB, the predicted Ebp base pilin, were not appreciably different from pili of OG1RF in our study. As overexpression of the major pilin has also been shown to increase pilus length (40), it is possible that the *ebpA* deletion affected relative EbpC levels.

We demonstrated that the deletion of either or both minor pilins reduced the proportion of piliated *E. faecalis* cells in a population by an unknown mechanism. Many sortase-assembled pilus islands include a divergently transcribed, upstream positive regulator, *ebpR* in the case of the *E. faecalis ebp* operon (41). Additionally, deletion of *rnjB*, a putative RNase J2, reduced pilus expression and levels of *ebpABC* mRNA transcript (42). Interestingly, it was recently reported that RrgA, the tip pilin of the *S. pneumoniae rlrA* pilus islet, interacts with RlrA, the upstream positive regulator of pilus expression, to exert a negative effect on population piliation dynamics of *S. pneumoniae* (43), presenting a mechanism whereby a structural pilin affected population piliation dynamics. Future studies will determine how the *ebpA* and *ebpB* deletions affected pilus biogenesis and whether they interacted with *ebpR* or *rnjB* to do so. Not surprisingly, the minor pilin deletion mutants (EbpA$^-$, EbpAB$^-$, and EbpB$^-$ strains), which all exhibited perturbed pilus biogenesis, were attenuated in experimental CAUTI.

Interestingly, the nonpiliated EbpC$^-$ mutant behaved similarly to OG1RF in experimental CAUTI, showing that the major polymerizing EbpC subunit and pilus fibers were dispensable for *E. faecalis* virulence. Similarly, the major subunits, but not the minor RrgA and Cpa tip pilins, were dispensable for pneumococcal mouse upper airway colonization (44) and GAS skin colonization in a humanized mouse model (27), respectively. Indeed, minor pilins expressed in the absence of pilus fibers have been shown to govern several sortase-assembled pilus functions *in vitro*, including adherence to cell lines and static biofilm formation (22, 44, 45). It has thus been suggested that pilus fibers serve to extend a minor functional pilin beyond the bacterial capsule where it can interact with host molecules (22). In this case, since OG1RF does not produce the *E. faecalis* capsular polysaccharide (46), EbpC pilus fibers, but not a functional minor subunit, would be dispensable for pilus function in OG1RF, just as we observed in experimental CAUTI.

Our analysis of minor pilin expression in *ebpC* and sortase mutants argued that a sortase-assembled EbpA-EbpB heterodimer was expressed in the absence of pilus fibers in the EbpC$^-$ strain. Similarly, the *C. diphtheriae* SpaC and SpaB minor pilins heterodimerized and anchored to the cell wall in the absence of the major pilin in a sortase-dependent fashion (47). The nonpiliated EbpAC$^-$, EbpBC$^-$, and SrtC$^-$ mutants that expressed mainly EbpA and/or EbpB monomers, but not the putative EbpA-EbpB heterodimer, were severely attenuated in experimental UTI, suggesting that sortase-assembled EbpA and/or EbpB mediated Ebp pilus function.

To directly test the importance of the minor pilins in CAUTI, we sought to create mutations in functional domains that did not affect pilus biogenesis. EbpA contains a predicted Cna B domain, not investigated here, and a VWA domain. VWA domains, named for their role in platelet adhesion to damaged vascular endothelium by the human plasma protein von Willebrand factor (48), are widely distributed among archaea, bacteria, and eukaryotes. Well-studied examples occur in some integrins, ECM proteins, and magnesium (Mg) chelatases and perform diverse functions, usually protein-protein interaction or cell adhesion (49). Coordination of a divalent cation by a MIDAS motif, present in almost half of all VWA domains, is critical for the function of some VWA domain-containing proteins (49). Most prokaryotic VWA domains have not been investigated in detail. However, Konto-Ghiorghi et al. showed that the GBS PilA tip pilin VWA domain was important for pilus-mediated bacterial adhesion to human alveolar and intestinal epithelial cells *in vitro* (22). Furthermore, the crystal structure of the pneumococcal RrgA tip pilin modeled an Mg^{2+} ion coordinated by the MIDAS motif of its VWA domain (50). We therefore hypothesized that EbpA's MIDAS motif would be important for Ebp pilus function in our model of CAUTI. Indeed, MIDAS motif mutants were as attenuated *in vivo* as were the relevant nonpiliated control strains, showing that an intact MIDAS motif is necessary for Ebp pilus function in bladder and implant colonization in experimental *E. faecalis* CAUTI. To our knowledge, this is the first study ascribing a sortase-assembled pilus function *in vivo* in a disease model to a specific protein domain. The importance of a MIDAS motif for the function of a prokaryotic VWA domain-containing protein has otherwise been shown only for the *Rhodobacter capsulatus* Mg chelatase BchD subunit (51), a member of an evolutionarily distinct family of VWA domain-containing proteins (49).

The functional role of the Ebp pilus governed by EbpA's VWA domain and MIDAS motif in bladder and implant colonization in experimental CAUTI remains to be determined. However, this function was tissue and model specific since pilin mutants colonized kidneys similarly to OG1RF in experimental CAUTI and both kidneys and bladders in our mouse model of ascending UTI. MIDAS motifs in the integrin beta and some alpha subunits are involved in integrin binding to ECM proteins (49). The VWA domain- and MIDAS motif-containing tip pilins RrgA and PilA have both been reported to bind ECM proteins such as collagen (26, 52). Furthermore, PilA's interaction with collagen is a critical component of GBS virulence in a mouse model of hemorrhagic meningitis (26). Crude cell wall extracts of a distinct nonpiliated *E. faecalis* mutant demonstrated reduced adherence to purified human collagens and fibrinogen compared to those of OG1RF, implicating Ebp pili in adhesion to these ECM molecules (33). Binding of bacteria to ECM proteins exposed by damage to vascular endothelium initiates infective endocarditis, an enterococcal disease in which Ebp pili are also implicated (8). In our CAUTI model, implantation leads to physiological changes in the bladder epithelium and induction of inflammation (32), potentially revealing host binding partners, such as ECM proteins, for recognition by EbpA. Colonization of implants may proceed by the same mechanism, as urinary catheters become coated with host proteins and components (53). Alternatively, EbpA's VWA domain may perform a distinct behavior that facilitates *in vivo* biofilm formation on implants. Polar *ebp* disruption mutants showed reduced static biofilm formation *in vitro* (8), suggesting that Ebp pili

may be involved in adherence to abiotic surfaces or bacterial surface components.

The diversity of bacterial species with sortase-assembled pili is matched only by the variety of potential niches and disease processes in which these pili function. However, a particular pilin or pilin domain is implicated for only a few of these behaviors. By mutating the predicted metal ion-coordinating amino acids of the MIDAS motif in EbpA's VWA domain, we preserved pilus biogenesis and showed a clear role for this motif in the function of the Ebp pilus *in vivo*. Future studies will determine whether the VWA domains of EbpA and other sortase-assembled tip pilins function similarly to those of the integrin subunits or other characterized MIDAS motif-containing VWA domains, allowing the development of structure-function correlates for pilus-mediated virulence in a wide variety of diseases.

MATERIALS AND METHODS

Bacterial strains and growth conditions. Bacterial strains are listed in Table S1 in the supplemental material. Unless otherwise noted, we grew *Escherichia coli* in Difco LB (Luria-Bertani) broth at 37°C with agitation and *E. faecalis* OG1RF (ATCC 47077) and its derivative strains statically at 37°C in Bacto BHI broth with rifampin (Rif; 25 to 100 μg ml^{-1}). Plasmid-containing strains were grown with appropriate antibiotics (see Table S2 in the supplemental material). For *E. coli*, erythromycin (Erm) was added at 500 μg ml^{-1}, kanamycin (Kan) at 50 μg ml^{-1} (25 μg ml^{-1} for pREP4), and ampicillin (Amp) at 100 μg ml^{-1}. For *E. faecalis*, Erm was added at 25 μg ml^{-1} and Kan at 500 μg ml^{-1}. All media were purchased from BD (Becton, Dickinson and Company, Franklin Lakes, NJ). Antibiotics were purchased from Sigma-Aldrich Corporation (St. Louis, MO).

General cloning techniques. DNA and amino acid sequences were retrieved and analyzed as described in Text S1 in the supplemental material. Bacterial genomic DNA (gDNA) was isolated with the Wizard Genome DNA purification kit (Promega Corp., Madison, WI). Plasmids are listed in Table S2 in the supplemental material. Aside from pABG5, pGCP123, and their derivatives, which were purified with the Hurricane Maxi Prep kit (Gerard Biotech LLC, Oxford, OH), plasmid DNA was isolated with the Wizard Plus SV Minipreps DNA purification system (Promega Corp.). Primers are listed in Table S3 in the supplemental material. PCR was performed with Phusion DNA polymerase from Finnzymes (Thermo Fisher Scientific, Inc., Rockford, IL). Site-directed mutagenesis (SDM) was carried out with QuikChange or QuikChange II kits (Stratagene, La Jolla, CA). Restriction endonucleases and T4 DNA ligase were purchased from New England Biolabs (Ipswich, MA). Ligations were transformed into *E. coli* TOP10, NovaBlue, or XL1-Blue cells. Plasmids derived here were confirmed by sequencing of inserts.

Generation of chromosomal deletion strains. Deletion of pilin coding sequences from the OG1RF chromosome was accomplished by allelic replacement as described previously using the temperature-sensitive shuttle vector pJRS233 (36). The Δ*ebpA*, Δ*ebpB*, Δ*ebpC* Δ*ebpAB*, Δ*ebpBC*, Δ*ebpABC*, Δ*ebpABCsrtC*, and Δ*srtC* deletion alleles comprised upstream (US) and downstream (DS) DNA fragments (~1,000 bp each) of the region to be deleted that were spliced by overlap extension PCR (SOE-PCR) (54). Single gene deletion alleles removed protein-coding open reading frame (ORF) sequences of the deleted gene only, preserving any overlapping ORF or intergenic sequence. Alleles for multiple gene deletions preserved any overlapping and intergenic sequence between remaining ORFs and deleted ORFs but removed any intergenic sequence between consecutively deleted ORFs. Table S4-A in the supplemental material details allele construction. Each allele was cloned into pJRS233 as described for each resultant plasmid listed in Table S2-G. When noted in Table S4-A, alleles were first blunt end ligated into a commercial vector. The EbpA$^-$, EbpB$^-$, EbpC$^-$, EbpAB$^-$, EbpBC$^-$, EbpABC$^-$, and SrtC$^-$ strains were created by transformation of OG1RF with pSJH-529, pSJH-530, pSJH-523, pSJH-531, pSJH-532, pSJH-524, and pSJH-189, respectively, by electroporation. The EbpAC$^-$, EbpABC$^-$ SrtC$^-$, and SrtC$^-$ SrtA$^-$ strains were created by transformation of EbpC$^-$, EbpABC$^-$, and SrtA$^-$ strains with pSJH-529, pSJH-279, and pSJH-189, respectively. Transformants were selected with Erm at 30°C and then passaged at the nonpermissive temperature (42°C) with Erm to select for chromosomal integration of the plasmid. Subsequent plasmid excision was allowed by passage at 30°C without Erm. Erm-sensitive colonies with double-crossover events that integrated deletion alleles were selected by PCR screening. Deletions were confirmed by PCR with gDNA.

Chromosomal MIDAS motif mutant construction. Mutation of EbpA's MIDAS motif on the OG1RF chromosome was accomplished by allelic replacement with the *ebpA*^{AWAGA} allele (coding for Ala^{315}-Trp-Ala^{317}-Gly-Ala^{319} in EbpA; see Table S4-B in the supplemental material) using pGCP213 instead of pJRS233. Creation of the pGCP213 temperature-sensitive shuttle vector is described in Text S1 in the supplemental material. The *ebpA*^{AWAGA} allele was introduced into pGCP213 as described for pSJH-509 in Table S2-H. An extraneous nucleotide added by primers HVN228 and HVN229 was deleted by SDM using primers HVN241 and HVN242, resulting in pSJH-509. OG1RF was transformed with pSJH-509 and passaged as described above. We screened for incorporation of the mutant allele by BspEI digestion of internal *ebpA* colony PCR products. A BspEI restriction site in the OG1RF allele is absent in the *ebpA*^{AWAGA} allele. The resultant EbpA^{AWAGA} chromosomal MIDAS motif mutant was confirmed by gDNA sequencing.

Generation of *E. faecalis* expression strains. Plasmids were created for expression of *ebp* genes in *trans* in *E. faecalis* using the Gram-positive expression vector pGCP123 (derived here as described in Text S1 in the supplemental material). All pGCP123 derivatives included the region 500 bp upstream of EbpA's translational start codon as the putative *ebpA* promoter (*ebpAp*). See Table S2-I for construction details of the following plasmids: pSJH-491 (p-*ebpABC*) encodes all structural pilins, pSJH-492 (p-*ebpAB*) encodes just EbpA and EbpB, pSJH-496 (p-*ebpABCsrtC*) encodes all structural pilins and SrtC, and pSJH-559 (p-*ebpA*^{AWAGA}*BCsrtC*) encodes the *ebpA*^{AWAGA} allele of EbpA and OG1RF alleles of EbpB, EbpC, and SrtC. EbpABC$^-$ and EbpABC$^-$ SrtC$^-$ strains were transformed with empty pGCP123 (see Table S1-C) and the plasmids derived above (see Table S1-D).

Generation of polyclonal antisera. Expression constructs for each Ebp pilin lacking the signal sequence and CWSS (EbpA-X, EbpB-X, and EbpCA-X) were created as described in Table S4-D in the supplemental material and cloned into the isopropyl-d-1-thiogalactopyranoside (IPTG)-inducible expression vector pQE-30Xa (Qiagen Inc., Valencia, CA), resulting in the addition of an N-terminal RGS-6×His tag. The EbpA-X construct comprised roughly the C-terminal half of EbpA. When noted in Table S4-D, constructs were first blunt end ligated into a commercial vector. The resultant pQE-30Xa-derived plasmids encoding recombinant EbpA, EbpB, and EbpC (pSJH-541, pSJH-547, and p-SJH-550, respectively) were used to transform the *E. coli* expression strain M15/pREP4 or SG13009/pREP4, resulting in strains SJH1987, SJH1988, and SJH1985. Text S1 describes the purification of recombinant EbpA, EbpB, and EbpC. Polyclonal antisera were generated commercially by immunization of New Zealand White rabbits with purified, recombinant EbpA or EbpB (New England Peptide, Gardner, MA) and by immunization of mice with purified, recombinant EbpC (Agro-Bio, La Ferté Saint-Aubin, France). Specificities of the immune sera were confirmed by a lack of signal on Western blots of cell lysates from the appropriate deletion mutants. No reactivity of preimmune sera to Ebp pili was observed on Western blots of OG1RF (data not shown).

Western blots. Bacterial cell fractions (prepared as described in Text S1 in the supplemental material) were boiled for at least 10 min in β-mercaptoethanol-containing loading buffer, and SDS-PAGE was performed with NuPAGE Novex 3 to 8% Tris-acetate gels in NuPAGE Tris-acetate SDS running buffer (Life Technologies Corp., Carlsbad, CA). Membranes were probed with antipilin sera as indicated and Pierce stabilized horseradish peroxidase-conjugated goat anti-rabbit or goat anti-

mouse IgG (Thermo Fisher Scientific, Inc.). Blots were developed with SuperSignal West Femto chemiluminescent substrate (Thermo Fisher Scientific, Inc.); film was processed with a Kodak X-Omat processor. Precision Plus Protein Kaleidoscope Standards (Bio-Rad Laboratories, Inc., Hercules, CA) are indicated. Distinct blots or exposures are separated by white space in the figures; lines represent an irrelevant gel lane that was removed using Adobe Photoshop CS2 (Adobe Systems Inc., Mountain View, CA).

IFM. IFM was performed as described previously (36). Slides were labeled with mouse anti-EbpC sera at a 1:1,000 dilution, Molecular Probes Alexa Fluor 594 anti-mouse IgG (Life Technologies Corp.), and Hoechst stain. Imaging was performed with AxioVision software and a Zeiss Axioskop 2 MOT Plus wide-field fluorescence microscope at the Department of Molecular Microbiology Imaging Facility of Washington University in St. Louis, MO. Quantification of EbpC-expressing cells is described in Text S1 in the supplemental material.

Deep-etch immunogold EM. Bacterial cells grown in TSBG (BBL Trypticase soy broth with 0.25% glucose) were deposited onto glass slides, fixed, and labeled as described previously (55) using mouse anti-EbpC sera and 18-nm gold bead-conjugated goat anti-mouse secondary antibody (Jackson ImmunoResearch Laboratories Inc., West Grove, PA). Samples were freeze-dried and imaged as described elsewhere (55, 56). The Shadows/Highlights function of Adobe Photoshop CS2 (Adobe Systems) was applied to Fig. 3E as a whole.

Negative-stain immunogold EM. Bacteria grown overnight were diluted 1:1,000 into TSBG and grown for ~14 h. Cells were harvested by centrifugation (5,000 × *g*, 5 min), washed in phosphate-buffered saline (PBS), and resuspended in PBS-5% calf serum. Cells were adsorbed to grids, labeled with anti-EbpC, negatively stained with uranyl acetate, and imaged as described previously (36) using goat anti-rabbit IgG conjugated to 18-nm colloidal gold particles (Jackson ImmunoResearch Laboratories).

Mouse model of CAUTI. All mouse CAUTI experiments were carried out in compliance with protocols approved by the Washington University in St. Louis Animal Studies Committee. C57BL/6 female mice purchased from the National Cancer Institute (Frederick, MD) were acclimated in our animal facility for 1 week. Experiments were performed with 7- to 8-week-old mice as described previously (32). Briefly, silicone implants were inserted transurethrally, and mice were infected with ~4×10^7 CFU (unless otherwise noted) of *E. faecalis*. Twenty-four hours or 7 days p.i., mice were sacrificed; bladders, kidneys, and implants were harvested; and bacterial burdens were determined by viable counting on Rif- and fusidic acid (Fus)-containing media. The CFU values of samples from which no colonies were recovered were set to the limit of detection. Samples from infections with plasmid-containing strains were also plated on Kan-containing media. No significant differences between the titers from Kan-containing and Kan-free media were observed (data not shown). Data from mice that lost their implant before sacrifice were excluded. Three to eight mice were included for each bacterial strain at each time point in each experiment.

Statistical analyses. Data from multiple experiments were pooled. Two-tailed Mann-Whitney *U* tests were performed with GraphPad Prism 5 software (GraphPad Software, San Diego, CA) for all comparisons described in CAUTI, ascending UTI, and IFM experiments. When noted in the figure legends, Bonferroni's adjustment for multiple comparisons was performed manually. An adjusted *P* value of <0.05 was considered statistically significant.

SUPPLEMENTAL MATERIAL

Supplemental material for this article may be found at http://mbio.asm.org/lookup/suppl/doi:10.1128/mBio.00177-12/-/DCSupplemental.

Figure S1, TIF file, 1.4 MB.
Figure S2, TIF file, 2.6 MB.
Text S1, PDF file, 0.3 MB.
Table S1, PDF file, 0.2 MB.
Table S2, PDF file, 0.2 MB.
Table S3, PDF file, 0.2 MB.
Table S4, PDF file, 0.1 MB.

ACKNOWLEDGMENTS

This work was supported by the NIDDK grant DK51406 and its ARRA supplement DK51406-12S1 awarded to S.J.H., the American Heart Association Midwest Affiliate Predoctoral Fellowship 10PRE2640099 to H.V.N., an ASM Robert D. Watkins Graduate Research Fellowship Award to P.S.G., and a W. M. Keck Postdoctoral Fellowship to G.C.P.

We thank D. K. Robertson, R. Roth, and J. E. Heuser for assistance with EM studies. We are grateful to K. W. Dodson for critical reading of the manuscript and to members of the Hultgren, Caparon, and Normark laboratories for helpful insight and discussion.

REFERENCES

1. **Murray BE.** 1990. The life and times of the enterococcus. Clin. Microbiol. Rev. **3**:46–65.
2. **Arias CA, Murray BE.** 2012. The rise of the *Enterococcus*: beyond vancomycin resistance. Nat. Rev. Microbiol. **10**:266–278.
3. **Edwards JR, et al.** 2009. National Healthcare Safety Network (NHSN) report: data summary for 2006 through 2008, issued December 2009. Am. J. Infect. Control **37**:783–805.
4. **Cope M, et al.** 2009. Inappropriate treatment of catheter-associated asymptomatic bacteriuria in a tertiary care hospital. Clin. Infect. Dis. **48**: 1182–1188.
5. **Wagenlehner FM, et al.** 2002. Epidemiological analysis of the spread of pathogens from a urological ward using genotypic, phenotypic and clinical parameters. Int. J. Antimicrob. Agents **19**:583–591.
6. **Warren JW, et al.** 1987. Fever, bacteremia, and death as complications of bacteriuria in women with long-term urethral catheters. J. Infect. Dis. **155**:1151–1158.
7. **Hidron AI, et al.** 2008. NHSN annual update: antimicrobial-resistant pathogens associated with healthcare-associated infections: annual summary of data reported to the National Healthcare Safety Network at the Centers for Disease Control and Prevention, 2006–2007. Infect. Control Hosp. Epidemiol. **29**:996–1011.
8. **Nallapareddy SR, et al.** 2006. Endocarditis and biofilm-associated pili of *Enterococcus faecalis*. J. Clin. Invest. **116**:2799–2807.
9. **Ton-That H, Schneewind O.** 2003. Assembly of pili on the surface of *Corynebacterium diphtheriae*. Mol. Microbiol. **50**:1429–1438.
10. **Mishra A, Das A, Cisar JO, Ton-That H.** 2007. Sortase-catalyzed assembly of distinct heteromeric fimbriae in *Actinomyces naeslundii*. J. Bacteriol. **189**:3156–3165.
11. **Lauer P, et al.** 2005. Genome analysis reveals pili in group B *Streptococcus*. Science **309**:105.
12. **Mora M, et al.** 2005. Group A *Streptococcus* produce pilus-like structures containing protective antigens and Lancefield T antigens. Proc. Natl. Acad. Sci. U. S. A. **102**:15641–15646.
13. **Barocchi MA, et al.** 2006. A pneumococcal pilus influences virulence and host inflammatory responses. Proc. Natl. Acad. Sci. U. S. A. **103**: 2857–2862.
14. **Budzik JM, Marraffini LA, Schneewind O.** 2007. Assembly of pili on the surface of *Bacillus cereus* vegetative cells. Mol. Microbiol. **66**:495–510.
15. **Sillanpää J, et al.** 2008. Identification and phenotypic characterization of a second collagen adhesin, Scm, and genome-based identification and analysis of 13 other predicted MSCRAMMs, including four distinct pilus loci, in *Enterococcus faecium*. Microbiology **154**:3199–3211.
16. **Hendrickx AP, et al.** 2008. Expression of two distinct types of pili by a hospital-acquired *Enterococcus faecium* isolate. Microbiology **154**: 3212–3223.
17. **Kankainen M, et al.** 2009. Comparative genomic analysis of *Lactobacillus rhamnosus* GG reveals pili containing a human-mucus binding protein. Proc. Natl. Acad. Sci. U. S. A. **106**:17193–17198.
18. **Foroni E, et al.** 2011. Genetic analysis and morphological identification of pilus-like structures in members of the genus *Bifidobacterium*. Microb. Cell Fact. **10**(Suppl. 1):S16. http://dx.doi.org/10.1186/1475-2859-10-16.
19. **Kline KA, Dodson KW, Caparon MG, Hultgren SJ.** 2010. A tale of two pili: assembly and function of pili in bacteria. Trends Microbiol. **18**: 224–232.
20. **Ton-That H, Schneewind O.** 2004. Assembly of pili in gram-positive bacteria. Trends Microbiol. **12**:228–234.

21. **Mandlik A, Das A, Ton-That H.** 2008. The molecular switch that activates the cell wall anchoring step of pilus assembly in gram-positive bacteria. Proc. Natl. Acad. Sci. U. S. A. **105**:14147–14152.
22. **Konto-Ghiorghi Y, et al.** 2009. Dual role for pilus in adherence to epithelial cells and biofilm formation in *Streptococcus agalactiae*. PLoS Pathog. **5**(5):e1000422. http://dx.doi.org/10.1371/journal.ppat.1000422.
23. **Paulsen IT, et al.** 2003. Role of mobile DNA in the evolution of vancomycin-resistant *Enterococcus faecalis*. Science **299**:2071–2074.
24. **Maisey HC, et al.** 2008. A group B streptococcal pilus protein promotes phagocyte resistance and systemic virulence. FASEB J. **22**:1715–1724.
25. **Papasergi S, et al.** 2011. The GBS PI-2a pilus is required for virulence in mice neonates. PLoS One **6**:e18747. http://dx.doi.org/10.1371/journal.pone.0018747.
26. **Banerjee A, et al.** 2011. Bacterial pili exploit integrin machinery to promote immune activation and efficient blood-brain barrier penetration. Nat. Commun. **2**:462. http://dx.doi.org/10.1038/ncomms1474.
27. **Lizano S, Luo F, Bessen DE.** 2007. Role of streptococcal T antigens in superficial skin infection. J. Bacteriol. **189**:1426–1434.
28. **Becherelli M, et al.** 2012. The ancillary protein 1 of *Streptococcus pyogenes* FCT-1 pili mediates cell adhesion and biofilm formation through heterophilic as well as homophilic interactions. Mol. Microbiol. **83**:1035–1047.
29. **Singh KV, Nallapareddy SR, Murray BE.** 2007. Importance of the *ebp* (endocarditis- and biofilm-associated pilus) locus in the pathogenesis of *Enterococcus faecalis* ascending urinary tract infection. J. Infect. Dis. **195**:1671–1677.
30. **Kemp KD, Singh KV, Nallapareddy SR, Murray BE.** 2007. Relative contributions of *Enterococcus faecalis* OG1RF sortase-encoding genes, *srtA* and *bps* (*srtC*), to biofilm formation and a murine model of urinary tract infection. Infect. Immun. **75**:5399–5404.
31. **Sillanpää J, et al.** 2010. Characterization of the ebp_{fm} pilus-encoding operon of *Enterococcus faecium* and its role in biofilm formation and virulence in a murine model of urinary tract infection. Virulence **1**:236–246.
32. **Guiton PS, Hung CS, Hancock LE, Caparon MG, Hultgren SJ.** 2010. Enterococcal biofilm formation and virulence in an optimized murine model of foreign body-associated urinary tract infections. Infect. Immun. **78**:4166–4175.
33. **Nallapareddy SR, Singh KV, Sillanpää J, Zhao M, Murray BE.** 2011. Relative contributions of Ebp pili and the collagen adhesin Ace to host extracellular matrix protein adherence and experimental urinary tract infection by *Enterococcus faecalis* OG1RF. Infect. Immun. **79**:2901–2910.
34. **Nallapareddy SR, et al.** 2011. Conservation of Ebp-type pilus genes among enterococci and demonstration of their role in adherence of *Enterococcus faecalis* to human platelets. Infect. Immun. **79**:2911–2920.
35. **El Mortaji L, Terrasse R, Dessen A, Vernet T, Di Guilmi AM.** 2010. Stability and assembly of pilus subunits of *Streptococcus pneumoniae*. J. Biol. Chem. **285**:12405–12415.
36. **Kline KA, et al.** 2009. Mechanism for sortase localization and the role of sortase localization in efficient pilus assembly in *Enterococcus faecalis*. J. Bacteriol. **191**:3237–3247.
37. **Lee JO, Rieu P, Arnaout MA, Liddington R.** 1995. Crystal structure of the A domain from the alpha subunit of integrin CR3 (CD11b/CD18). Cell **80**:631–638.
38. **Kau AL, et al.** 2005. *Enterococcus faecalis* tropism for the kidneys in the urinary tract of C57BL/6J mice. Infect. Immun. **73**:2461–2468.
39. **Swaminathan A, et al.** 2007. Housekeeping sortase facilitates the cell wall anchoring of pilus polymers in *Corynebacterium diphtheriae*. Mol. Microbiol. **66**:961–974.
40. **Swierczynski A, Ton-That H.** 2006. Type III pilus of corynebacteria: pilus length is determined by the level of its major pilin subunit. J. Bacteriol. **188**:6318–6325.
41. **Bourgogne A, et al.** 2007. EbpR is important for biofilm formation by activating expression of the endocarditis and biofilm-associated pilus operon (*ebpABC*) of *Enterococcus faecalis* OG1RF. J. Bacteriol. **189**:6490–6493.
42. **Gao P, et al.** 2010. *Enterococcus faecalis rnjB* is required for pilin gene expression and biofilm formation. J. Bacteriol. **192**:5489–5498.
43. **Basset A, et al.** 2011. Expression of the type 1 pneumococcal pilus is bistable and negatively regulated by the structural component RrgA. Infect. Immun. **79**:2974–2983.
44. **Nelson AL, et al.** 2007. RrgA is a pilus-associated adhesin in *Streptococcus pneumoniae*. Mol. Microbiol. **66**:329–340.
45. **Mandlik A, Swierczynski A, Das A, Ton-That H.** 2007. *Corynebacterium diphtheriae* employs specific minor pilins to target human pharyngeal epithelial cells. Mol. Microbiol. **64**:111–124.
46. **Thurlow LR, Thomas VC, Hancock LE.** 2009. Capsular polysaccharide production in *Enterococcus faecalis* and contribution of CpsF to capsule serospecificity. J. Bacteriol. **191**:6203–6210.
47. **Chang C, Mandlik A, Das A, Ton-That H.** 2011. Cell surface display of minor pilin adhesins in the form of a simple heterodimeric assembly in *Corynebacterium diphtheriae*. Mol. Microbiol. **79**:1236–1247.
48. **Sadler JE.** 1998. Biochemistry and genetics of von Willebrand factor. Annu. Rev. Biochem. **67**:395–424.
49. **Whittaker CA, Hynes RO.** 2002. Distribution and evolution of von Willebrand/integrin A domains: widely dispersed domains with roles in cell adhesion and elsewhere. Mol. Biol. Cell **13**:3369–3387.
50. **Izoré T, et al.** 2010. Structural basis of host cell recognition by the pilus adhesin from *Streptococcus pneumoniae*. Structure **18**:106–115.
51. **Lundqvist J, et al.** 2010. ATP-induced conformational dynamics in the AAA+ motor unit of magnesium chelatase. Structure **18**:354–365.
52. **Hilleringmann M, et al.** 2008. Pneumococcal pili are composed of protofilaments exposing adhesive clusters of RrgA. PLoS Pathog. **4**(3):e1000026. http://dx.doi.org/10.1371/journal.ppat.1000026.
53. **Habash M, Reid G.** 1999. Microbial biofilms: their development and significance for medical device-related infections. J. Clin. Pharmacol. **39**:887–898.
54. **Horton RM, Cai ZL, Ho SN, Pease LR.** 1990. Gene splicing by overlap extension: tailor-made genes using the polymerase chain reaction. BioTechniques **8**:528–535.
55. **Hanson PI, Roth R, Lin Y, Heuser JE.** 2008. Plasma membrane deformation by circular arrays of ESCRT-III protein filaments. J. Cell Biol. **180**:389–402.
56. **Heuser JE, et al.** 1979. Synaptic vesicle exocytosis captured by quick freezing and correlated with quantal transmitter release. J. Cell Biol. **81**:275–300.